INFLUENCE OF FORMATION CONDITIONS, SUBSEQUENT ANNEALING AND ION IRRADIATION ON THE PROPERTIES OF NANOSTRUCTURED COATINGS BASED ON AMORPHOUS CARBON WITH GOLD, SILVER AND NITROGEN ADDITIVES[†]

Aleksandr Kolpakov[a], Aleksandr Poplavsky[a,b], Maksim Yapryntsev[a],
Vseslav Novikov[a], Sergey Manokhin[c], Igor Goncharov [a,b],
Marina Galkina [a,b], Vyacheslav Beresnev[d,*]

[a]*Belgorod National Research University, 308015 Belgorod, Russia*
[b]*Belgorod State Technological University Named After V.G. Shoukhov, 308012, Belgorod, Russia*
[c]*Institute of Problems of Chemical Physics, Russian Academy of Sciences, 142432, Chernogolovka, Russia*
[d]*V.N. Karazin Kharkiv National University Svobody Sq. 4, 61022, Kharkiv, Ukraine*
Corresponding Authors: v.beresnev@karazin.ua; novikov_v@bsu.edu.ru
Received June 14, 2021; revised July 27, 2021; accepted July 29, 2021

Nanostructured coatings based on amorphous carbon and carbon-doped with gold, silver, and nitrogen were obtained by the pulsed vacuum-arc method. Carbon coatings have been annealed in a vacuum as well as treated with argon ions. The alloying of carbon coatings with elements that do not form chemical bonds with the carbon matrix (Ag, Au) leads to the formation of gold or silver nanocrystallites with sizes of 2 - 20 nm in the matrix of amorphous carbon, whose density depends on the concentration of the doping element. Annealing of silver-doped carbon coatings leads to the formation of islands on the surface with the size of the order of micrometers. This is due to the silver diffusion and coalescence of small islands into larger ones. The HRTEM method discovered the effect of twinning in carbon nanocrystallites after vacuum annealing as well as silver and gold in the initial state (the formation of single-crystal regions with an altered orientation of the crystal structure) in the amorphous carbon matrix. Analysis of Raman spectra of pure carbon coating and silver-doped showed that the addition of silver leads to a decrease in sp3-phase in the carbon matrix. This effect is particularly evident in the nature of changes in the spectra after vacuum annealing at 600 ºC. The addition of nitrogen in the carbon coating leads to an increase in the sp2 - phase fraction, and additional annealing leads to a significant increase in the D - peak intensity and formation of clusters of the order of 5 - 15 nm, which are not localized but fill the entire space. Analysis of the coating a-C: Au irradiation with argon ions shows that the number of nanopitches decreased after ion irradiation, simultaneously decreased surface roughness degree, besides, decreased electrical conductivity of the coating as a result of decreased gold content. It was found that the conditions of nanostructured coatings and their subsequent processing allow controlling the properties of nanocoatings (structure, size of nanoparticles, surface topography, and electrical conductivity).

Keywords: Nanostructured coatings, Amorphous carbon, Alloying, Gold, Silver, Nitrogen, Annealing
PACS: 61.66.f, 61.46w

The peak of studies of coatings based on superhard carbon (mainly DLC) falls at the end of the twentieth and beginning of the twenty-first century. Several reviews are devoted to this object [1,2]. Despite the frustrations associated with the main drawbacks of DLC coatings (high internal stresses and defectiveness), their potential is far from being exhausted both in scientific terms [3] and in terms of purely applied research. According to Dr. Vetter [4], who has published the most objective and detailed review devoted to the history of these coatings and their many applications, this area of research should not be retired. One promising area of development of this research could be the creation of DLC-based nanostructures, which significantly expand the applications of these coatings.

According to the publications [5,6], solid DLC coatings obtained on a cold substrate by deposition of carbon particles with an energy of the order of 20-100 eV have a disordered quasiamorphic structure, and their properties approach the properties of the diamond as the content of the phase with sp3 hybridization of carbon atoms increases. Such coatings have come to be classified as ta-C. At present, attempts are being made to study more finely the structure of these coatings; in particular, nanoclusters with sizes on the order of 2.5 nm have been found in carbon coatings obtained by laser sputtering of a graphite target [7].

According to the data of [8] annealing in a vacuum at 600 °C allows initiating the formation of nanocrystallites with an ordered structure in the amorphous matrix of ta-C coatings. It was found that the size of nanocrystallites depends on the initial state of the carbon matrix and, first of all, on the content of the sp3 phase and the level of internal stresses in it, which is determined by the conditions of coating formation.

Another method of forming nanostructures based on the amorphous carbon matrix is the addition of elements that do not form stable chemical bonds with carbon atoms (Au, Ag, Pt, Cu) to the coating. Several studies have reported the detection of nanoclusters of these metals in the matrix of amorphous carbon [9,10]. In [11] using high-resolution HRTEM electron microscopy nanoclusters with an ordered structure (silver nanocrystallites with sizes of

the order of 10-50 nm) were found. It was found that the size of nanocrystallites depends on the conditions of coating formation.

Other method of nanostructured state formation is the creation of nanolayers based on DLC coatings with different densities by changing the energy of carbon ions arriving at the substrate [12]. In this case, layers with preferential growth in a certain direction are created.

The addition of nitrogen to the carbon coating formed by the pulsed vacuum-arc method and its subsequent annealing to increase the electrical conductivity leads to the formation of nanoclusters with sizes of the order of 3-10 nm [13]. At the same time, the structure of the coating is radically different from that obtained by annealing ta-C coatings [8], namely, the formation of local areas of nanocrystallites is not observed.

The state of the substrate, namely, the presence of defects in the initial state or created by directed actions, for example, ion bombardment or laser irradiation, allows changing the conditions of coating formation. In this regard, the peculiarities of nanostructured coating formation based on a matrix of amorphous carbon and silver nanoparticles on a substrate of NaCl single crystal can be noted. The effect of substrate defects in the form of steps and dislocation yield on the density and size of silver nanoparticles has been detected [11].

The subsequent processing of the coating is of particular interest. In [14] a nanocomposite thin coating containing gold nanoparticles in a carbon matrix (Au/a-C) was obtained on glass substrates by co-sputtering in a high-vacuum chamber. To increase the size of Au nanoparticles, thermal annealing of the deposited coatings was performed at temperatures ranging from 100 to 500 °C in an inert argon atmosphere. The growth of Au nanoparticles and the evolution of the carbon matrix during thermal treatment were investigated by PEM and Raman spectroscopy. PEM images of the deposited sample taken at different sections of the studied sample revealed spherical Au nanoparticles with an average diameter of 1.5 nm, whose size increases to 15.3 nm at a temperature of 500 °C.

A promising method of surface modification is irradiation with accelerated ions, which causes several physical processes (surface sputtering, ion implantation, formation of radiation defects) that can be used for etching, alloying with various elements, and accelerating diffusion processes [15,16].

Thus, the purpose of this work is to find common approaches to the formation of the nanostructured state of carbon-based coatings and to determine the possibility of comprehensive use of the above methods of subsequent processing to expand their areas of application.

EXPERIMENTAL PROCEDURE

Nanoscale carbon coatings 100-300 nm thick were deposited on an experimental setup equipped with a pulsed carbon plasma source of the original design (Fig. 1).
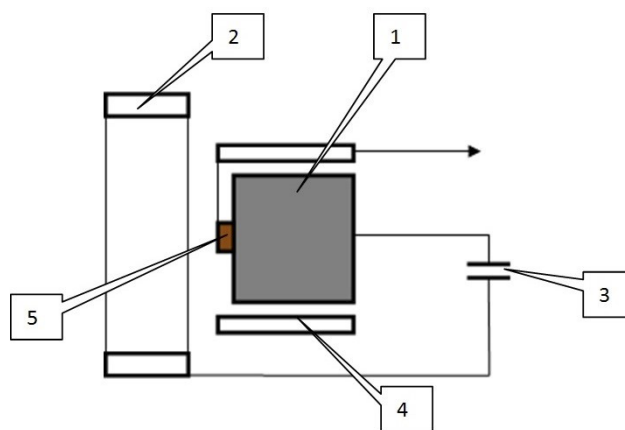
Figure 1. Pulsed carbon plasma source
1 - graphite cathode; 2 - anode; 3 - capacitive storage; 4 - ignition electrode; 5 - ignition assembly insulator

Carbon plasma source consists of graphite cathode 1 and ring anode 2, which are connected to the capacitive storage unit 3 with the capacitance of 2000 µF, charged from DC source to 300 V (not shown in Figure 1). The discharge is initiated between cathode 1 and anode 2 by applying a high-voltage pulse between the ignition electrode 4 and cathode 1, resulting in spark breakdown of the insulator surface 5 with excitation of cathode spots on cathode 1. Carbon coatings with silver and gold were applied using a similar pulsed plasma source equipped with a graphite cathode with silver and gold inserts. The firing pulse repetition rate was 1-5 Hz. Discharge pulse duration was set within the range of 0.8-1.0 ms. The productivity of this source was 0.6-0.7 nm/imp at 100 mm from the cathode.

For structural studies, coatings with a thickness of about 100 nm were deposited on polished plates of monocrystalline silicon and on a fresh chipped NaCl monocrystal. The coatings deposited on the NaCl monocrystal were separated from the substrate in distilled water according to the standard procedure.

The coatings were annealed in the Carbolite vacuum furnace GHA 10/600 at 600 °C for 10 minutes. At the same time, it took 40 minutes to reach the specified temperature mode. The samples were removed from the furnace the next

day after they had cooled completely. The subsequent irradiation was performed by argon ions with an energy of 1.0 keV. The internal stresses were determined before and after annealing by the laser-optical method based on the substrate deflection.

Carbon coatings with nitrogen addition were obtained in the modes indicated above, but with simultaneous irradiation with nitrogen ions at an energy of about 700 eV according to the procedure described in detail in [13]. The monocrystalline silicon substrate was previously degreased and placed in a vacuum chamber, which was evacuated to a pressure of $1 \cdot 10^{-3}$ Pa. Before coating, the substrate was treated with argon ions using an electron-ion source with a closed electron drift at a discharge voltage of 2.0 kV and a discharge current of 80 mA for 3 minutes. The coating thickness was set by the number of discharge pulses and determined preliminarily on crosssection chips using a QUANTA 600 FEG scanning electron microscope.

The surface morphology was studied using scanning electron microscopes QUANTA 600 and Nova NanoSEM 450 as well as a scanning probe microscope NTEGRA AURA. The elemental composition of the a-CN coatings was determined by X-ray microanalysis on a scanning electron microscope.

Structural studies were performed on a high-resolution Tecnai G2 F20 S-TWIN transmission electron microscope. To calculate the average particle size, histograms of horizontal and vertical secant size distributions were plotted for each of the samples. Then, the average histogram was plotted, from which the average particle size was determined. Raman spectra were obtained using a LabRAM HR Evolution spectroscope (laser wavelength 532 nm, power 50 mW).

RESULTS
Carbon coating

Figure 2 shows a dark-field PEM image of the carbon coating in the initial state and after annealing in a vacuum at 600 °C. There is a significant difference between the structure of the coatings in the initial state and after annealing. The coating structure in the initial state is amorphous and close to homogeneous. The internal stresses in the initial state are 12 GPa.

After annealing, local bright areas appear on the PEM images, half of which have a size of 10 to 20 nm according to the histogram of their size distribution (Fig. 3). The value of internal stresses after annealing decreases to 2 GPa.
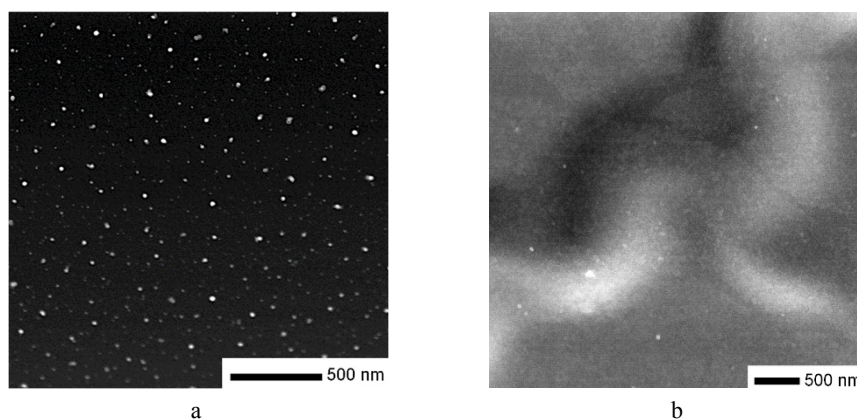
Figure 2. Dark-field PEM image of the carbon coating in the initial state (a) and after annealing in vacuum at 600 °C (b).
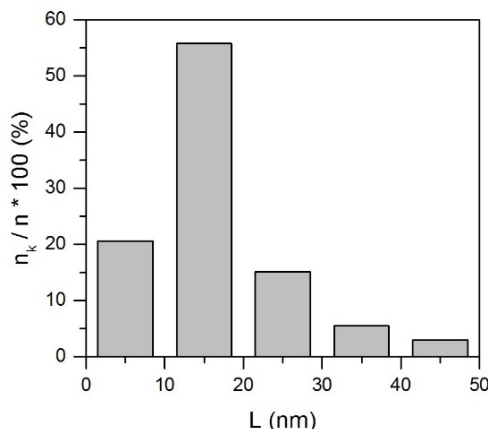
Figure 3. Histogram of the size distribution of local light regions for the carbon coating after annealing in vacuum at 600 °C.

Fig. 4 shows HRTEM images of light regions of different sizes in the amorphous matrix. The analysis of the light regions showed that they are nanosized crystallites with a HCC structure. The interplanar distances are 2.47 Å, 2.13 Å, and 1.51 Å. The calculated value of the lattice parameter was 4.27±0.01 Å, and the unit cell volume was 0.78 Å3 (note

that the unit cell volume of a diamond is 0.45 Ǻ3). It can be seen that areas of larger size are an agglomeration of several crystallites, indicated by arrows in Fig. 4b.

The plasmon energies obtained from the electron energy loss spectra for the samples in the initial state and after annealing are 30 eV and 30.5 eV.

Figure 5 shows the Raman spectra of the coating in the initial state and after annealing in a vacuum at 600 °C. It can be seen that the Raman spectra before and after annealing are almost identical, only the main G peak is observed. A more detailed analysis of these spectra by decomposition into the constituent D and G peaks showed the absence of structural changes in the sp2 phase during annealing.

a   b
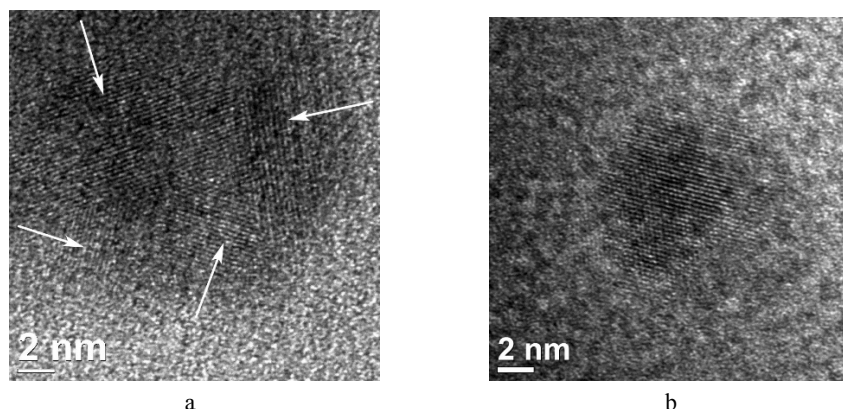
Figure 4. HRTEM-images of light regions in the carbon coating structure after annealing at 600 °C in a vacuum. Single nanocluster (a) and a cluster of nanocrystallites (b).
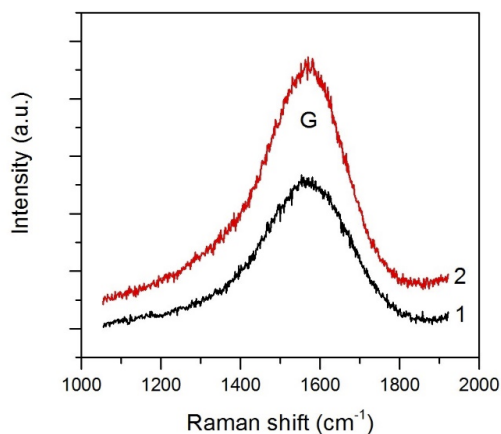
Figure 5. Raman spectra of the coating in the initial state (1) and after annealing in a vacuum at 600 °C (2).

Silver-doped carbon coating

Fig. 6a shows the picture of electron diffraction of carbon coating with silver additives (a-C:Ag), and in Fig. 6b its dark-field PEM image. The silver content in the coating is 10 at.%. Diffraction rings correspond to interplanar distances of crystalline silver (ring number - interplanar distance,Å: 1 – 2.36, 2 – 2.04, 3 – 1.45, 4 – 1.24).

a   b
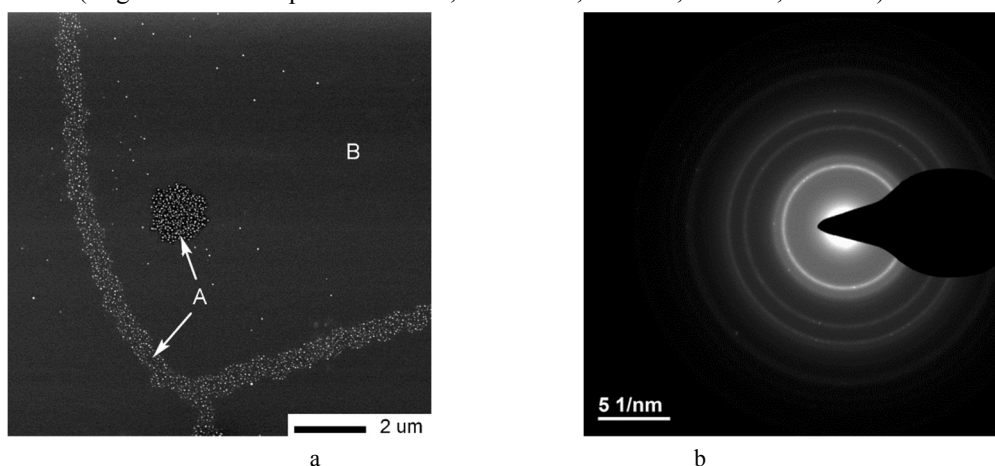
Figure 6. Coating a-C:Ag, electron diffraction (a), dark-field PEM image (b).

It was found that silver atoms are grouped into individual clusters, which are silver nanocrystallites. Their distribution density and size are determined by substrate defects and internal stresses occurring in the coating matrix. For example, silver nanocrystallites in the A region are much larger than those in the dark B region (Figure 6b). A single silver nanocrystallite is shown in Figure 7. It has face-centered cubic lattice (HCC), and the calculated interplanar distances and lattice parameters agree well with the tabulated data for silver.
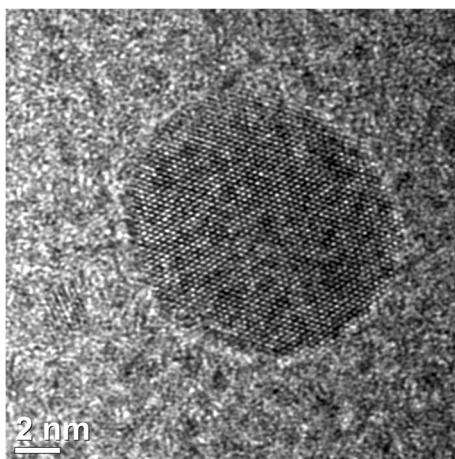
Figure 7. HRTEM images of silver nanocrystallite in the carbon matrix.

Figure 8a shows the appearance of the surface of a-C:Ag coating after annealing at 600 °C obtained by scanning electron microscopy. After annealing silver agglomeration from the coating volume into large objects with the size of 1 - 5 microns on the surface is observed.

Figure 8b shows the Raman spectra of silver-doped carbon coatings in the initial state and after annealing in vacuum at 600 °C. The intensity of the Raman spectrum of the coating after annealing increases significantly. This can be explained by the reduction of the surface reflection coefficient as a result of silver agglomeration from the coating volume into large objects. The development of the D - peak (about 1350 cm-1) indicates the formation of sp2 clusters in the carbon matrix.

a   b
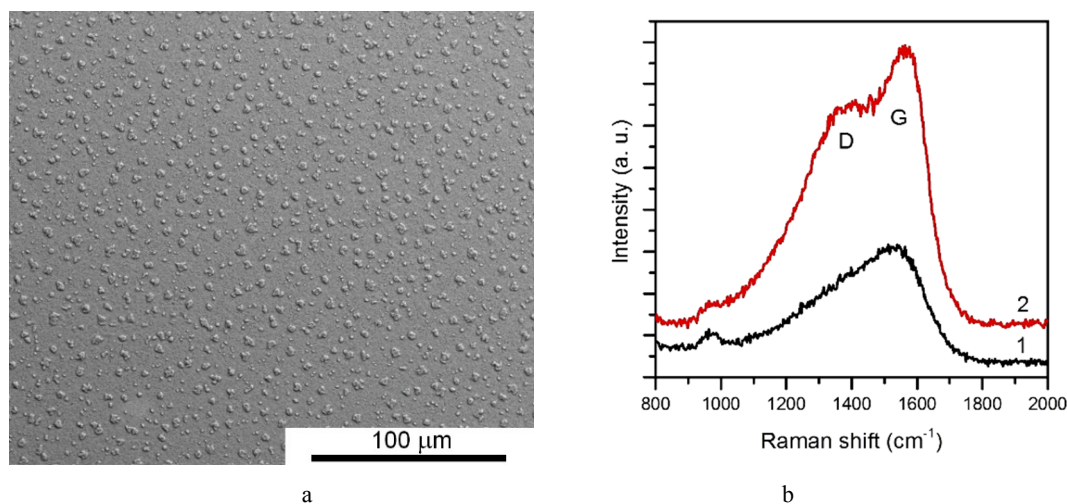
Figure 8. (a) - Surface appearance of a-C:Ag coating after annealing at 600 °C, (b) - Raman spectra of a-C:Ag coating in the initial state (1) and after annealing at 600 °C (2)

Nitrogen-doped carbon coating

Figure 9 shows a PEM image of a nitrogen-doped (a-C:N) carbon coating after annealing at 600 °C (a) and a histogram of the sp2 cluster size distribution. In the dark-field image of the sample taken in the region of the 1st ring distribution of electron diffraction, the contrast characteristic of nanoscale phases is observed. No such bright features were observed prior to annealing. Analysis of the image, as well as the histogram, allows us to conclude that the structure of the a-C:N coating differs significantly from ta-C (see Figs. 2,3,4) after annealing.

The Raman spectra are shown in Figure 10 also differ dramatically, both in the initial state and after annealing. Annealing at 600 °C has no effect on the Raman spectrum intensity. The increase in the D peak intensity and the shift of the G peak position towards higher wavenumbers are related to the growth of sp2 clusters in the carbon matrix. This indicates the evolution of the amorphous carbon matrix towards nanocrystalline graphite.

a   b
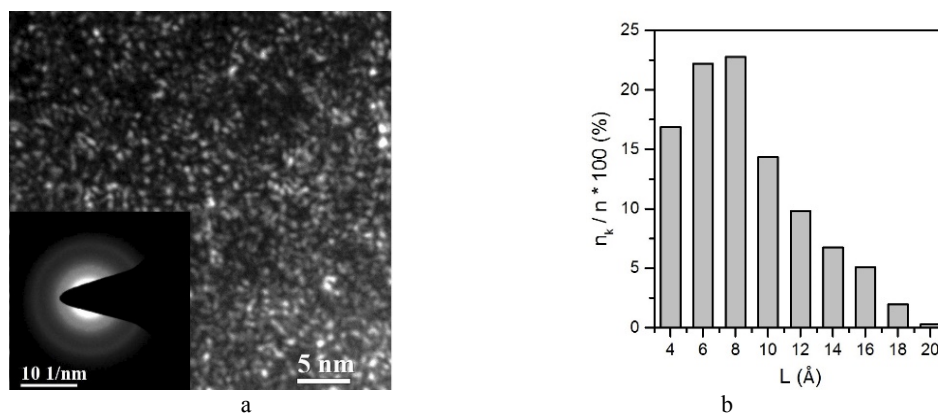
Figure 9. TEM image of a-C: N carbon coating after annealing at 600 ° C (a) and histogram of the cluster size distribution (b)
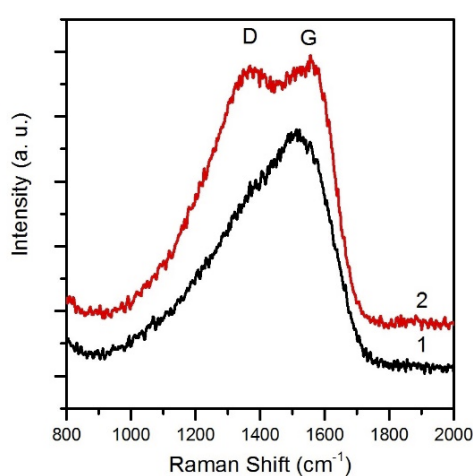
Figure 10. Raman spectra of a-C:N coating in the initial state (1) and after annealing (2)

Gold-doped carbon coating

Samples of carbon coatings with different concentrations of gold (a-C:Au) from 1 to 26 at.% were obtained, and everywhere the grouping of gold atoms into nanosized particles of globular morphology is observed. Figure 11 shows an electron microscopic image of a carbon coating with 18 at.% gold content and an electron diffraction pattern. The diffraction rings correspond to the gold structure (ring number - interplanar distance, Å: 1 - 2.30, 2 - 2.07, 3 - 1.41, 4 - 1.20). HRTEM study of individual particles also showed that their lattice parameters correspond to the known from literature values of gold (cubic face-centered lattice, spatial group Fm-3m, lattice parameters a = b = c = 4.08 Å) When fusing of two or more crystal individuals observed twinning effect (Fig. 12a). The histogram of gold particle size distribution is shown in Fig. 12b. The density of gold nanocrystallites increases with increasing of gold content.

a   b
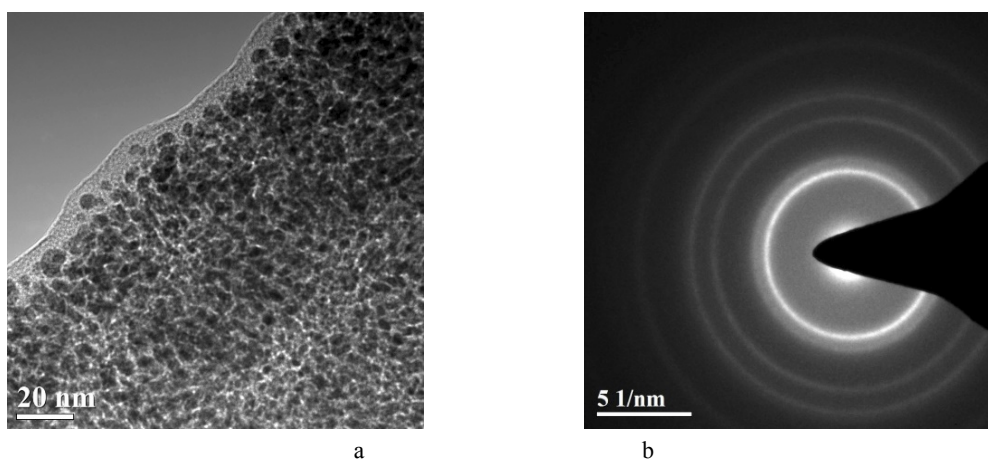
Figure 11. Electron microscopic image of carbon coating with 18 at.% gold (a) and its electron diffraction pattern (b)

a
b
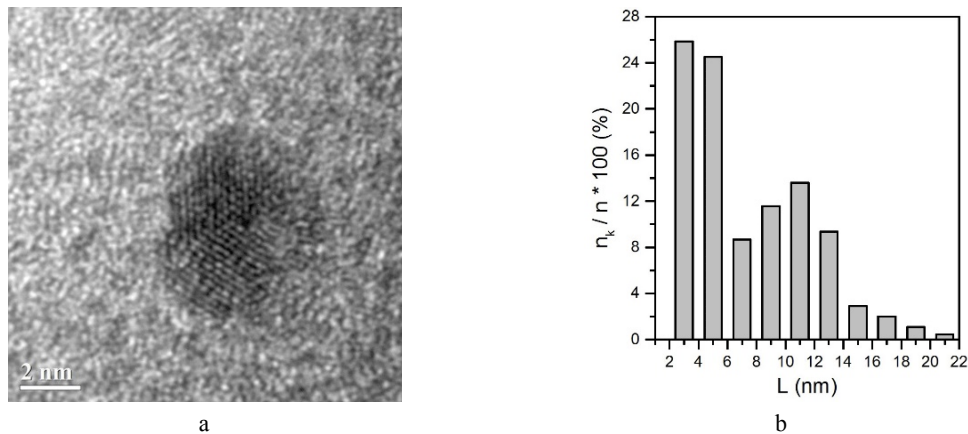
Figure 12. HRTEM image of gold nanocrystallite with the twinning effect (a) and histogram of the gold particle size distribution (b)

Figure 13 shows scans of the a-C:Au coating surface obtained by AFM in the initial state (a) and after irradiation with argon ions (b) at an energy of 1 keV for 10 min. After ion irradiation, the average surface roughness decreased from 21 nm to 10 nm.

a
b
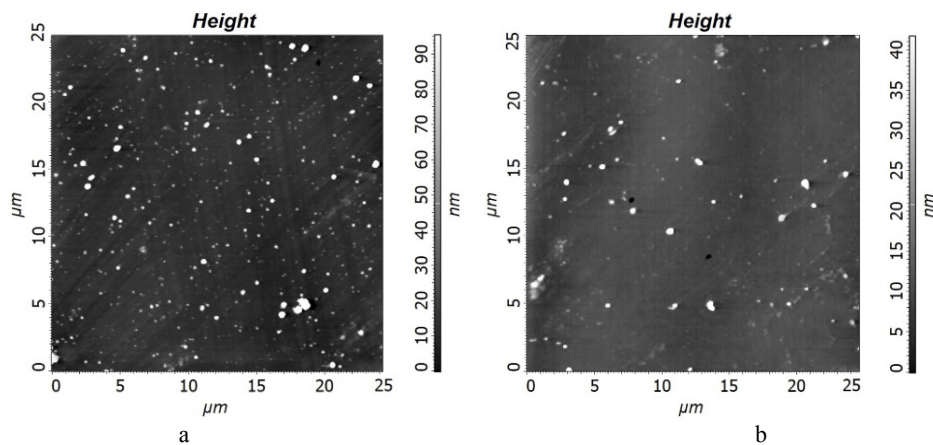
Figure 13. AFM scans of the a-C:Au coating surface in the initial state (a) and after irradiation with argon ions (b) at an energy of 1 keV for 10 min

To assess the electrical conductivity of the a-C:Au coating surface before and after the ion irradiation, we used the technique of determining the resistance of the flow-through, for which a potential of 1 V was applied to the probe. The results of scanning in this mode are shown in Fig. 14.

Analyzing the results of these scans, we can note that the number of nano increases decreased after ion irradiation, while the degree of surface roughness decreased. In addition, the electrical conductivity of the a-C:Au coating (see Fig. 14) decreased as a result of the reduction of the gold content from 26% to 10%.

a
b
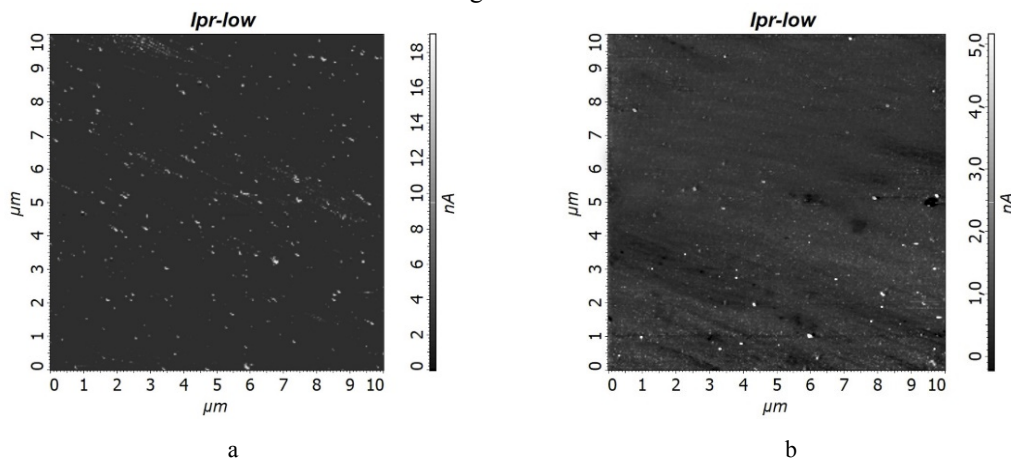
Figure 14. Scans of a-C:Au coating surface in the mode of determination of the flow resistance in the initial state (a) and after irradiation with argon ions with the energy of 1 keV for 10 min (b)

Figure 15 shows an electron microscopic image of the a-C:Au coating surface after etching with argon ions at 1 keV energy for 20 minutes. The initial gold content in the coating is 10%, and after ion etching, it approaches zero. The dark areas on the surface are most likely craters left by the etching of the gold particles.
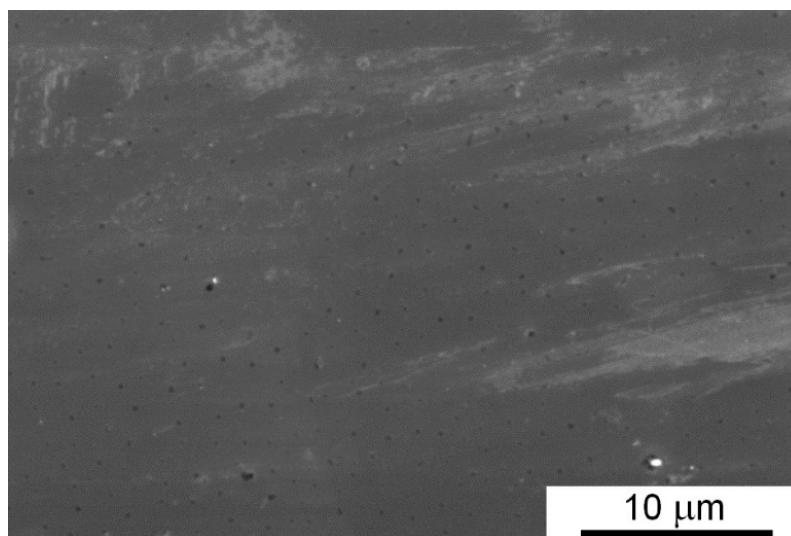
Figure 15. Electron microscopic image of a-C:Au coating surface after etching with argon ions at an energy of 1 keV for 20 minutes

ANALYSIS OF THE RESULTS

Analyzing the HRTEM images shown in Figure 4, it should be noted that a feature of the ordered regions formed during annealing is that they consist of several nanocrystallites (shown by arrows in Figure 4b). In addition, the crystallites are formed in the [011] direction of the GCC lattice, perpendicular to the coating surface. The size of the nanocrystallites after annealing depends on the initial value of internal stresses and increases as the value of internal stresses increases, which in turn is determined by the number of radiation defects.

It is known that the study by EELS (electron energy-loss spectroscopy) method allows determining the ratio of phases with different hybridization of valence electrons (sp3, sp2) [17]. Plasmon energy value determined by this technique is related to the local density of valence electrons and correlates with the density of carbon coating. The plasmon energy values for diamond, DLC-coating, and graphite are 34 eV, 30 eV, and 27 eV, respectively [18]. Annealing of the coating leads to a slight increase in the plasmon energy. Consequently, we can conclude that annealing of DLC coatings deposited by the pulsed vacuum-arc method leads not to graphitization of the coating structure, but to partial ordering in the coating structure. This conclusion is confirmed by the identity of the Raman spectra of the coating in the initial state and after annealing in a vacuum at a temperature of 600 °C, shown in Fig. 5. It is especially necessary to note the increase of the plasmon energy to the value of 30.5 eV, which may indicate an increase in the coating density after annealing, which may be one of the reasons for the decrease in the value of internal stresses.

It was found that large silver nanoclusters are formed predominantly in the dislocation exit sites and steps on the NaCl monocrystal surface. The nucleation energy of nanoclusters is lower in these defective sites and favorable conditions for coalescence of smaller clusters into larger ones. Thus, the state of the substrate surface significantly affects the size and density of silver nanoclusters.

The analysis of the Raman spectra of the pure carbon coating and silver-doped one showed that the addition of silver leads to a decrease in the sp3-phase content in the carbon matrix, which coincides with the results of other publications. This effect is particularly evident in the nature of changes in the spectra after vacuum annealing at a temperature of 600 ºC.

The addition of nitrogen to the carbon coating leads to an increase in the sp2 - phase, and additional annealing to a significant increase in the intensity of the D - peak and the formation of clusters with sizes of about 5 - 15 nm, which are not localized but fill the entire space in contrast to ta-C - coating after the same annealing [8]. At the same time, the clusters in a-C:N -coating do not have an ordered structure. The element composition of the a-C:N coating is preserved after annealing, which indicates the absence of significant diffusion of elements to the natural sinks (surface and transition zone) [13].

The analysis of the results of the irradiation of the a-C:Au coating with argon ions allows us to conclude that the number of nanosteaks decreased after ion irradiation, the degree of surface roughness simultaneously decreased, and, in addition, the electrical conductivity of the coating decreased as a result of the decrease in the gold content. To explain this result, we used the simulation of the interaction of argon ions with gold and amorphous carbon targets in the SRIM program environment [19]. It was found that the sputtering coefficient of the gold target significantly exceeds the corresponding value for amorphous carbon (3.726 atom/ion and 0.218, respectively). Thus, the preferential etching of gold nanoparticles occurs.

CONCLUSIONS

Annealing of amorphous carbon coatings ta-C with a high level of internal stresses leads to the formation of nanocrystallites with preferential sizes of 10 - 20 nm, which is associated with a high concentration of radiation defects and their migration in the fields of internal stresses.

The alloying of carbon coatings with elements that do not form chemical bonds with the carbon matrix (Ag, Au) leads to the formation of gold or silver nanocrystallites with sizes of 2 - 20 nm in the matrix of amorphous carbon, whose density depends on the concentration of the alloying element.

The state of the substrate surface (surface energy) significantly affects the size of silver nanocrystallites and their density, which can be used to visualize surface defects.

The effect of twinning in carbon nanocrystallites after vacuum annealing as well as silver and gold in the initial state (formation of areas with the changed orientation of the crystal structure in the monocrystal) in the matrix of amorphous carbon was detected by the HRTEM method.

Annealing of silver-doped carbon coatings leads to the formation of islands on the surface with the size of the order of micrometers. This is due to the diffusion of silver and coalescence of small islands into larger ones.

The addition of nitrogen to the carbon coating leads to an increase in the proportion of sp2 - phase, and additional annealing to the formation of clusters with sizes of the order of 5 - 15 nm, which are not localized but fill the entire space in contrast to the ta-C coating after the same annealing. The clusters in the a-C:N coating do not have an ordered structure.

The irradiation of the surface of the carbon coating with gold addition by argon ions leads to a decrease in its roughness and electrical conductivity, which is associated with the preferential etching of gold nanoparticles. Increasing the dose of ion irradiation leads to the complete etching of gold nanoparticles, which can be used in the future for the formation of nanomembranes based on amorphous carbon.

ORCID ID

Aleksandr Kolpakov, https://orcid.org/0000-0003-4836-5677; **Aleksandr Poplavsky**, https://orcid.org/0000-0001-6127-5874;
Maksim Yapryntsev, https://orcid.org/0000-0001-8791-8102; **Vseslav Novikov**, https://orcid.org/0000-0002-3602-0746;
Sergey Manokhin, https://orcid.org/0000-0002-1683-5614; **Igor Goncharov**, https://orcid.org/0000-0002-7734-0535;
Marina Galkina, https://orcid.org/0000-0003-0819-3153; **Vyacheslav Beresnev**, https://orcid.org/0000-0002-4623-3243

REFERENCES

[1]   Alfred Grill, Diam. Relat. Mater. **8**, 428 (1999). https://doi.org/10.1016/S0925-9635(98)00262-3
[2]   J. Robertson, Mater. Sci. Eng. R, **37**, 129 (2002). https://doi.org/10.1016/S0927-796X(02)00005-0
[3]   A.C. Ferrari, S.E. Rodil, J. Robertson, and W.I. Milne, Diam. Relat. Mater. **11**, 994, (2002). https://doi.org/10.1016/S0925-9635(01)00705-1
[4]   J. Vetter, Surf. Coat. Technol. **257**, 213 (2014). https://doi.org/10.1016/j.surfcoat.2014. 08.017
[5]   S. Xu, B.K. Tay, H.S. Tan, L. Zhong, Y.Q. Tu, S.R.P. Silva, and W.I. Milne, J. Appl. Phys. **79**, 7234 (1996). https://doi.org/10.1063/1.361440
[6]   D.R. McKenzie, D. Muller, B.A. Pailthorpe, Z.H. Wang, E. Kravtchinskaia, D. Segal, P.B. Lukins, P.D. Swift, P.J. Martin, G. Amaratunga, P.H. Gaskell, and A. Saeed, Diam. Relat. Mater. **1**, 51, (1991). https://doi.org/10.1016/0925-9635(91)90011-X
[7]   V.A. Plotnikov, B.F. Dem'yanov, A.P. Yeliseeyev, S.V. Makarov, and A.I. Zyryanova, Diam. Relat. Mater. **91**, 225 (2019). https://doi.org/10.1016/j.diamond.2018.11.022
[8]   A.Ya. Kolpakov, A.I. Poplavsky, M.E. Galkina, S.S. Manokhin, and J.V. Gerus, Appl. Phys. Lett. **105**, 233110 (2014). https://doi.org/10.1063/1.4903803
[9]   R.J. Narayan, H. Abernathy, L. Riester, C.J. Berry, R. Brigmon, J. of Materi Eng and Perform. **14**, 435 (2005). https://doi.org/10.1361/105994905X56197
[10] A.S. Chaus, T.N. Fedosenko, A.V. Rogachev, L. Čaplovič, Diam. Relat. Mater. **42**, 64 (2014). https://doi.org/10.1016/j.diamond.2014.01.001
[11] A.Ya. Kolpakov, A.I. Poplavsky, S.S. Manokhin, M.E. Galkina, I.Yu. Goncharov, R.A. Liubushkin, J.V. Gerus, P.V. Turbin, and L.V. Malikov, J. Nano- Electron. Phys. **8**(4), 04019 (2016). https://doi.org/10.21272/jnep.8(4(1)).04019
[12] M.B. Taylor, D.W.M. Lau, J.G. Partridge, D.G. McCulloch, N.A. Marks, E.H.T. Teo, and D.R. McKenzie. J. Phys.: Condens. Matter. **21**, 225003 (2009). https://doi.org/10.1088/0953-8984/21/22/225003
[13] A. Poplavsky, Yu. Kudriavtsev, A. Kolpakov, E. Pilyuk, S. Manokhin, and I. Goncharov, Vacuum, **184**, 109919 (2021). https://doi.org/10.1016/j.vacuum.2020.109919
[14] Ritu Vishnoi, Kshipra Sharma, Ganesh D. Sharma, and Rahul Singhal, Vacuum, **167**, 40 (2019). https://doi.org/10.1016/j.vacuum.2019.05.031
[15] *Ion Beam Modification of Solids: Ion-Solid Interaction and Radiation Damage*, (Switzerland: Springer International Publishing: 2016). https://doi.org/10.1007/978-3-319-33561-2
[16] Carsten Bundesmann, and Horst Neumann, J. Appl. Phys. **124**, 231102 (2018). https://doi.org/10.1063/1.5054046
[17] R.F. Egerton, Rep. Prog. Phys. **72**, 016502 (2008). https://doi.org/10.1088/0034-4885/72/1/016502
[18] J. Kulik, Y. Lifshitz, G.D. Lempert, E. Grossman, J.W. Rabalais, D. Marton, J. Appl. Phys. **76**, 5063 (1994). https://doi.org/10.1063/1.357218
[19] J.F. Ziegler, M.D. Ziegler, J.P. Biersack, Nuclear Instruments and Methods in Physics Research B, **268**, 1818 (2010). https://doi.org/10.1016/j.nimb.2010.02.091

ВПЛИВ УМОВ ФОРМУВАННЯ, ВІДПАЛУ ТА ІОННОГО ОПРОМІНЕННЯ НА ВЛАСТИВОСТІ НАНОСТРУКТУРНИХ ПОКРИТТІВ НА ОСНОВІ АМОРФНОГО ВУГЛЕЦЮ З ДОБАВКАМИ ЗОЛОТА, СРІБЛА ТА АЗОТУ

Олександр Колпаков[a], Олександр Поплавский[a,b], Максим Япрінцев[a], Всеслав Новіков[a], Сергій Манохин[a], Ігор Гончаров[a,b], Марина Галкіна[a,b], Вячеслав Береснєв[g]

[a]Бєлгородський національний дослідницький університет, 308015, Бєлгород, Росія
[b]Бєлгородський державний технологічний університет імені В.Г. Шухова, 308012, Бєлгород, Росія
[c]Інститут проблем хімічної фізики Російської академії наук, 142432, Черноголовка, Росія
[d]Харківський національний університет імені В.Н. Каразіна, 61022, Харків, Україна

Імпульсним вакуумно-дуговим методом сформовані наноструктурні покриття на основі аморфного вуглецю та вуглецю, легованого золотом, сріблом і азотом. Проведено відпал покриттів у вакуумі, а також обробка іонами аргону. Легування вуглецевих покриттів елементами, що не утворюють хімічних зв'язків з вуглецевою матрицею (Ag, Au) призводить до виділення нанокристалітів золота або срібла з розмірами 2 - 20 нм в матриці аморфного вуглецю, густина цих виділень залежить від концентрації легуючого елементу. Відпал вуглецевих покриттів, легованих сріблом, призводить до утворення на поверхні острівців металу з розмірами порядку мікрометру. Це пов'язано з дифузією срібла і коалесценцією малих острівців до утворення більших за розмірами. Методом HRTEM виявлений ефект двійникування в нанокристалітах вуглецю після відпалу в вакуумі, а також срібла та золота у вихідному стані (утворення в монокристалі областей зі зміненою орієнтацією кристалічних граток) в матриці аморфного вуглецю. Аналіз спектрів Рамана чистого вуглецевого покриття і легованого сріблом показав, що добавка срібла призводить до зменшення вмісту sp^3-фази в вуглецевій матриці. Найбільше цей ефект проявляється в характері зміни спектрів після вакуумного відпалу при температурі 600 ºC. Додавання азоту до вуглецевого покриття призводить до збільшення частки sp^2-фази, а додатковий відпал – до значного збільшення інтенсивності D-піку і формування кластерів з розмірами близько 5 - 15 нм, що не є локалізованими, а заповнюють весь об'єкт. Аналіз опромінення покриття a-C:Au іонами аргону свідчить про зменшення кількості нановиступів після іонного опромінення, одночасно зменшується ступінь шорсткості поверхні, а також електропровідність покриття (це є наслідком зменшення вмісту золота). Технологічні чинники формування наноструктурних покриттів і їхньої подальшої обробки дають можливість керувати властивостями нанопокриттів (структурою, розміром наночастинок, рельєфом поверхні і електропровідністю).

Ключові слова: наноструктурні покриття, аморфний вуглець, легування, золото, срібло, азот, відпал.